Lawrence Berkeley National Laboratory
Recent Work

Title

Indication from Precision Electroweak Physics Confront Theoretical Bounds on the Mass of the Higgs Boson

Permalink

Author

Ellis, J.

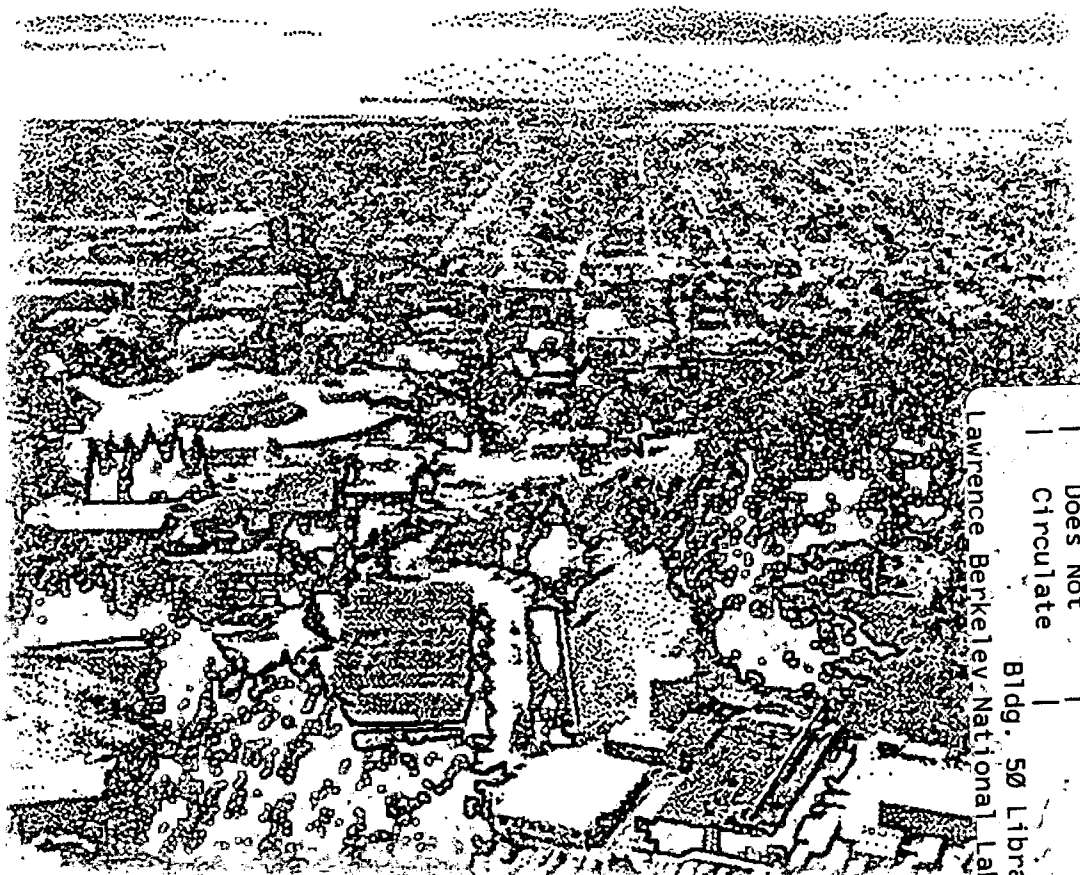**Publication Date**

1996-08-01

ERNEST ORLANDO LAWRENCE
BERKELEY NATIONAL LABORATORY

Indications from Precision Electroweak Physics Confront Theoretical Bounds on the Mass of the Higgs Boson

J. Ellis, G.L. Fogli, and E. Lisi
Physics Division

DISCLAIMER

Indications from Precision Electroweak Physics Confront Theoretical Bounds on the Mass of the Higgs Boson

John Ellis

CERN
CH-1211, Geneva, Switzerland

G.L. Fogli and E. Lisi

Dipartimento di Fisica and Sezione INFN di Bari
Bari, Italy

August 1996

Indications from Precision Electroweak Physics

Confront Theoretical Bounds on the Mass of the Higgs Boson

John Ellis*

CERN, CH-1211, Geneva, Switzerland

G. L. Fogli and E. Lisi

Dipartimento di Fisica and Sezione INFN di Bari, Bari, Italy

Abstract

An updated fit to the precision electroweak data and to the direct measurement of the top quark mass m_t provides significant constraints on m_t and on the Higgs boson mass M_H: $m_t/\text{GeV} = 172 \pm 6$ and $\log_{10}(M_H/\text{GeV}) = 2.16 \pm 0.33$, with an error correlation $\rho = 0.5$. We integrate the (M_H, m_t) probability distribution found in this analysis over various zones of the (M_H, m_t) plane defined by one-sided experimental and theoretical bounds on the Higgs boson mass, both in the Standard Model and in its minimal supersymmetric extension. The comparison of the cumulative probabilities gives interesting information on the likelihood that the true value of M_H is compatible with different theoretical scenarios.

The possibility of constraining *both* the top quark mass m_t *and* the Higgs boson mass M_H through their virtual effects on precision electroweak observables was recognized long ago [1]. The continuous refinement of the experimental measurements at the CERN Large Electron Positron Collider (LEP) and elsewhere has resulted in sustained improvement of these "indirect" bounds on m_t and M_H, both in the Standard Model (SM) [2, 3, 4, 5, 6, 7] and in the Minimal Supersymmetric extension of the Standard Model (MSSM) [8, 9, 10, 11, 12]. The predictive power of the precision electroweak data was confirmed dramatically by the "direct" determination of the top quark mass by the CDF [13] and D0 [14] experiments at the Tevatron, which currently yield $m_t = 175 \pm 6$ GeV (as reported in [15]). Combining these measurements with the precision electroweak data enables the corresponding prediction of M_H to be improved significantly [16, 17, 18].

A new stage has recently been attained with the release of preliminary new data from LEP, including almost all the data taken with Phase 1 of LEP around the Z^0 peak. The most recent available electroweak precision data from LEP and SLC are reported in [15]. In this paper, we first update our previous analyses of the precision electroweak data, combining the new data with the older low-energy precision data as described in [16]. We then confront the resulting fit with one-sided experimental and theoretical bounds on M_H in the Standard Model and the MSSM. The experimental bounds come from unsuccessful direct searches for the standard or supersymmetric Higgs boson at LEP 1 [19, 20]. Theoretical bounds in the Standard Model come from requiring its validity up to some large scale Λ, below which the current electroweak vacuum is assumed to be metastable [21], and renormalization group evolution does not cause the Standard Model couplings to diverge [22, 23]. Theoretical bounds within the MSSM come from calculations of the mass of the lightest neutral Higgs boson, including quantum corrections [24]. These bounds divide the (M_H, m_t) plane into several regions, depending on their consistency or otherwise with the Standard Model and/or the MSSM.

We use the joint probability distribution of (M_H, m_t) provided by our new global fit to estimate the relative (cumulative) probabilities that the true values of M_H and m_t lie within

each of these different regions. This enables us to estimate the likelihood that the true values of M_H and m_t will turn out to be compatible with the Standard Model and/or the MSSM. There is at present no significant difference between the likelihoods of the Standard Model and the MSSM, but a refinement of this type of analysis with future improvements in the precision electroweak data set has the potential to provide some discrimination between these models.

We start by reporting the result of a global analysis within the SM of the precision electroweak data recently made available, excluding initially the direct m_t determination. Our fitting program also includes all available lower-energy precision data, along the lines described in [16]. It now yields

$$m_t/\text{GeV} = 157^{+16}_{-12} \ , \tag{1}$$

$$\log_{10}(M_H/\text{GeV}) = 1.81^{+0.45}_{-0.36} \ , \tag{2}$$

where the errors on both m_t and $\log_{10}(M_H/\text{GeV})$ are at the 1-σ level. The information on M_H is quoted on a logarithmic scale, because electroweak observables characteristically exhibit a logarithmic dependence on M_H, and the probability distribution we find is closer to being Gaussian in $\log_{10}(M_H/\text{GeV})$. The corresponding numerical values of M_H at the 1-σ level are $M_H = 65^{+117}_{-37}$ GeV. We recall that this estimate of M_H was obtained without using the CDF and D0 measurements of m_t. It is consistent with the indications for a light Higgs mass obtained in our previous works [16, 9], as well as in [11, 17].

The estimate (1) of m_t is less than 1-σ below the direct measurement by the CDF and D0 collaborations: $m_t = 174 \pm 6$ GeV. This agreement constitutes dramatic confirmation of the SM at the one-loop level. It also justifies combining [16, 9] the indirect and direct measurements of m_t, which has the effect of readjusting the previous best-fit range (1) to higher values of m_t. The well-known positive m_t-M_H correlation in the radiative corrections then causes the best-fit value of M_H to increase as well:

$$m_t/\text{GeV} = 172 \pm 6 \ , \tag{3}$$

$$\log_{10}(M_H/\text{GeV}) = 2.16 \pm 0.33 \ . \tag{4}$$

We observe that the error in $\log(M_H)$ is now somewhat reduced and more symmetrical, and that the combined probability distribution is approximated to a good accuracy by a bivariate Gaussian in the variables $x = \log_{10}(M_H/\text{GeV})$ and $y = m_t/\text{GeV}$. This best-fit Gaussian distribution, that will be used hereafter, is completely defined by the 1-σ errors in Eqs. (3) and (4) and by their correlation, which in our fit is $\rho_{xy} = 0.5$. The 1-σ range (4) corresponds to $M_H = 145^{+164}_{-77}$ GeV. The results of our global fit are in good agreement with those recently reported by the LEP Electroweak Working Group [15].

The joint bounds on (x, y) in the MSSM do not differ appreciably from those in the SM, as long as the the MSSM spectrum is sufficiently heavy to be decoupled [9, 16]. We assume the MSSM parameters $m_{\tilde{g}} = m_0 = -\mu = 1$ TeV in the following (notation as in [10]), so that this decoupling is enforced. Subleading terms in the radiative corrections induce small differences between the MSSM and the SM only at low values of M_H, which are anyway disfavored by the probability distribution of M_H itself [Eq. (4)]. These observations indicate that, given the present information, it is reasonable to use the same (x, y) probability distribution in the SM and MSSM, subject to the different one-sided experimental and theoretical bounds that we discuss now.

In Fig. 1 we show the 1-σ and 2-σ contours ($\Delta\chi^2 = 1, 4$) of the joint probability distribution in the plane ($\log M_H$, m_t) (solid ellipses), together with experimental and theoretical one-sided bounds applicable in the Standard Model. The vertical hatched line represents the LEP lower bound $M_H > 65$ GeV [19]. The sloping curves on the left represent the lower limits on M_H coming from the requirement of 'metastability' of the electroweak vacuum [21]: their slopes reflect the dependence of this type of bound on m_t. The different curves correspond to the requirement that our present electroweak vacuum have a lifetime exceeding 10^{10} years for any transition to a lower-lying state with a Higgs expectation value $|H| \leq \Lambda$, according to calculations with the renormalization group improved effective potential. The curves on the right represent the upper limits on M_H derived by Lindner [22] from the 'triviality' requirement that none of the SM couplings should become singular at any renormalization scale $\mu \leq \Lambda$. Taken together, these two sets of lines represent the

4

requirement that the SM remain consistent at all scales below Λ. We observe that, for any given value of Λ, there is only a relatively narrow vertical band, narrowing at high m_t, which is allowed in Fig. 1 by the theoretical and experimental bounds.

In order to infer any useful information about the relative likelihoods that the true values of $(\log M_H, m_t)$ will be consistent with different values of Λ, it is necessary to take into account the joint $(\log M_H, m_t)$ probability distribution, as shown in Fig. 2.

In Fig. 2 we report the integrated (cumulative) probability in the region of the $(\log M_H, m_t)$ *excluded* by LEP, by vacuum metastability, and by triviality. The complementary fraction of probability gives the cumulative probability that the true value of $(\log M_H, m_t)$ lies in the allowed region. This exercise is repeated for different values of Λ. We notice that the LEP bound excludes only 15% of the total probability, providing the non-trivial information that the global fit to the precision electroweak data is statistically consistent with the negative results of the searches for the Higgs boson at LEP. On the other hand, the metastability bound excludes a significant fraction of the probability, unless $\Lambda \simeq 10^4$ GeV. In this case the metastability bound only excludes a zone which is already almost completely forbidden by the LEP searches (see Fig. 1). The triviality bounds also exclude a fraction of the probability which increases with Λ. The remaining allowed region is weighted by a cumulative probability which decreases from 77% at low Λ to 27% at high $\Lambda \simeq 10^{19}$ GeV.

Since the area of the $(\log M_H, m_t)$ plane that is allowed for large Λ is included within that allowed for small Λ, it is inevitable that the cumulative probability decrease monotonically with Λ. If the decrease is gradual, no useful information about the likelihood of different values of Λ can be extracted, whereas a precipitous decrease would indicate that some range was highly disfavored. We see from Fig. 2 that current data do not exclude statistically any value of Λ. However, according to the available information, it is about three times more likely that the true values of $(\log M_H, m_t)$ are consistent with a Standard Model valid up to a scale of 10^4 GeV than up to the Planck scale. This is an interesting piece of information that will become more specific as further constraints are placed on $(\log M_H, m_t)$, culminating in

the eventual direct measurement of M_H.

In Fig. 3 we study analogous constraints in the MSSM. In this case, the LEP lower limit on M_H varies with the ratio of supersymmetric Higgs vacuum expectation values, $\tan\beta$ [20]. The upper theoretical bound on M_H [24] also varies with $\tan\beta$ as well as with m_t. We do not show in Fig. 3 the lower theoretical bound on M_H, which is always below the LEP bounds.

In Fig. 4 we show the cumulative probabilities obtained by integrating the differential $(\log M_H, m_t)$ distribution in the various zones of Fig. 3. This exercise is repeated for different values of $\tan\beta$, and we see that a large fraction of the probability is excluded by the upper theoretical bound. This is a consequence of the best-fit value of M_H, which is at the limits of the allowed region in Fig. 3. No value of $\tan\beta$ can be statistically excluded, and we have not explored the quality of fits away from the decoupling limit of large sparticle mass parameters. However, it currently appears more likely that the true values of $(\log M_H, m_t)$ are consistent with a MSSM with high $\tan\beta$ ($\gtrsim 8$) than with $\tan\beta \simeq 1$.

It has been noticed [25, 26] that the bounds on M_H in the SM and MSSM define some zones in the $(\log M_H, m_t)$ plane where only one of the models (either the SM or the MSSM) is allowed. In other zones the SM and MSSM are both consistent, and the discovery of a Higgs boson would not help to discriminate between the models. We have made an exploratory calculation of the cumulative probabilities that the true values of $(\log M_H, m_t)$ lie in each of these zones, as shown in an SM-MSSM "phase diagram" in Fig. 5 for the particular cases $\Lambda = 10^{19}$ GeV and $\tan\beta = 4$.

In Fig. 5, the zone labelled 1 is bounded by the LEP lower limit on M_H in the MSSM. Zone 2 is bounded by this limit and by the LEP lower limit on M_H in the SM. Zones 3, 4, 5 and 6 are bounded by the strongest of the upper or lower SM or MSSM theoretical constraints. Zone 7 is excluded by triviality in the SM. The current probabilities that, according to the most complete available information, the true values of $(\log M_H, m_t)$ lie in each of the various zones are also indicated. Apart from zone 7, the two regions that appear most likely are 3 and 6, within which the SM and MSSM can be distinguished. Zone

6

3 corresponds to values of M_H that are above the LEP limit for the SM Higgs *but* below the SM vacuum metastability bound, *though* below the MSSM upper bound. Zone 6 corresponds to values of M_H allowed in the SM but above the upper limit imposed in the MSSM.

The zones in which the SM is consistent are 4 and 6, and we estimate a cumulative probability of 27% that the true values of $(\log M_H, m_t)$ lie within one or the other of these zones. The zones in which the MSSM is consistent are 2, 3, and 4, and we estimate a cumulative probability of 32% that the true values of $(\log M_H, m_t)$ lie within one of these zones. Note that the likelihood of the MSSM zones is not lower than that of the SM zones, even though the central value of M_H lies well inside the region of Fig. 1 that is consistent with the SM. Clearly, both the SM and the MSSM are highly consistent with the present data, which cannot be said to favour either of them in a significant way.

Looking to the future, however, there is the prospect that improvements in the precision electroweak data set, in particular greater accuracy in the M_W measurement [27], could provide some useful indication one way or the other. Also, any direct measurement of M_H may well resolve the issue. However, this is not guaranteed, since there is a region in Fig. 5, namely zone 4, where measured values of M_H and m_t would be consistent with both the SM and the MSSM. The cumulative probability that the true value of (M_H, m_t) lie in this zone (around 5%) is not completely negligible.

In conclusion: we have analysed the most complete available information from precision electroweak measurements to determine the (M_H, m_t) probability distribution. We have used the best-fit Gaussian approximation to this distribution to evaluate the cumulative probability that the true values of (M_H, m_t) are consistent with the experimental and theoretical one-sided bounds on M_H, both in the SM and in MSSM. Both the SM and the MSSM are consistent with the available data and the known constraints.

REFERENCES

[1] J. Ellis and G. L. Fogli, Phys. Lett. B **249** (1990) 543.

[2] J. Ellis, G. L. Fogli, and E. Lisi, Phys. Lett. B **274** (1992) 456.

[3] J. Ellis, G. L. Fogli, and E. Lisi, Phys. Lett. B **318** (1993) 148.

[4] F. del Aguila, M. Martinez, and M. Quirós, Nucl. Phys. B **381** (1991) 451.

[5] V. A. Novikov, L. B. Okun, M. I. Vysotski, and V. P. Yurov, Phys. Lett. B **308** (1993) 123.

[6] K. Hagiwara, S. Matsumoto, D. Haidt, and C. S. Kim, Z. Phys. C **64** (1994) 559; *ibidem* C **68** (1995) 352(E).

[7] G. Montagna, O. Nicrosini, G. Passarino, and F. Piccinini, Phys. Lett. B **335** (1994) 484.

[8] J. Ellis, G. L. Fogli, and E. Lisi, Phys. Lett. B **286** (1992) 85.

[9] J. Ellis, G. L. Fogli, and E. Lisi, Phys. Lett. B **333** (1994) 118.

[10] J. Ellis, G. L. Fogli, and E. Lisi, Nucl. Phys. B **393** (1993) 3.

[11] P. H. Chankowski and S. Pokorski, Phys. Lett. B **366** (1996) 188.

[12] W. de Boer, A. Dabelstein, W. Hollik, and W. Mösle, Karlsruhe University Report No. KA-TP-18-96, hep-ph/9607286.

[13] CDF Collaboration, F. Abe *et al.*, Phys. Rev. Lett. **74** (1995) 2676.

[14] D0 Collaboration, S. Abachi *et al.*, Phys. Rev. Lett. **74** (1995) 2632.

[15] A. Blondel, Plenary talk at the International Conference on High Energy Physics, Warsaw, 1996, reporting the analysis of the LEP Electroweak Working Group and the SLD Heavy Flavor Group, CERN Report No. LEPEWWG/96-02, available at the URL: http://www.cern.ch/LEPEWWG .

[16] J. Ellis, G. L. Fogli, and E. Lisi, Z. Phys. C **69** (1996) 627.

[17] P. H. Chankowski and S. Pokorski, Phys. Lett. B **356** (1995) 307; see also the update, hep-ph/9509207.

[18] S. Matsumoto, Mod. Phys. Lett. A **10** (1995) 2553.

[19] Particle Data Group, R. M. Barnett *et al.*, Phys. Rev. D **54** (1996) 1.

[20] J.F. Grivaz, Rapporteur talk given at *HEP '95*, International Europhysics Conference on High Energy Physics, Brussels, Belgium, 1995.

[21] J. R. Espinosa and M. Quirós, Phys. Lett. B **353** (1995) 257.

[22] M. Lindner, Z. Phys. C **31** (1986) 295.

[23] M. Sher, Phys. Rept. **179** (1989) 273.

[24] Y. Okada, M. Yamaguchi and T. Yanagida, Progr. Theor. Phys. **85** (1991) 1; J. Ellis, G. Ridolfi and F. Zwirner, Phys. Lett. B **257** (1991) 83 and B **262** (1991) 477; H. E. Haber and R. Hempfling, Phys. Rev. Lett. **66** (1991) 1815.

[25] M. A. Diaz, T. A. ter Veldhuis, and T. J. Weiler, Phys. Rev. Lett. **74** (1995) 2876; see also the updated version, Vanderbilt University Report No. VAND-TH-94-14-UPD, hep-ph/9512229; P. Q. Hung and M. Sher, Phys. Lett. B **374** (1996) 138.

[26] J. R. Espinosa, DESY Report No. 96-107, hep-ph/9606316, Lecture at *ITEPWS '96*, XXIV ITEP Winter School of Physics, to appear in the Proceedings.

[27] K. Kang and S. K. Kang, talk at "Beyond the Standard Model IV," Granlibakken, Lake Tahoe, California (1994), hep-ph/9503478.

FIGURES

FIG. 1. Indirect bounds on (M_H, m_t) and one-sided experimental and theoretical limits in the Standard Model. The solid ellipses represent the 1-σ and 2-σ contours from the best-fit Gaussian distribution obtained by analysing all electroweak precision data, including the measurement of m_t at CDF and D0. The hatched line is the LEP lower bound on M_H [19]. The other curves represent the lower and upper limits on M_H from vacuum metastability [21] and triviality [22, 23] respectively, as functions of the scale of new physics Λ.

FIG. 2. Cumulative (integrated) probabilities in the various zones excluded or allowed in the Standard Model by one-sided bounds. No value of Λ can be excluded.

FIG. 3. Indirect bounds on (M_H, m_t) and one-sided experimental and theoretical limits in the Minimal Supersymmetric Standard Model. Apart from the Higgs sector, the MSSM spectrum is assumed to be decoupled. Solid ellipses represent the 1-σ and 2-σ contours as in Fig. 1. The vertical lines are the LEP lower bounds on M_H [20], which depend slightly on $\tan\beta$. The other curves represent the upper limits on M_H in the MSSM [24], as a function of $\tan\beta$.

FIG. 4. Cumulative (integrated) probabilities in the various zones excluded or allowed in the Minimal Supersymmetric Standard Model by one-sided bounds. No value of $\tan\beta$ can be excluded.

FIG. 5. Superposition of SM and MSSM bounds in the (M_H, m_t) plane, for $\Lambda = 10^{19}$ GeV and $\tan\beta = 4$. The various zones 1–7 define regions that are (not) compatible with a SM or a MSSM Higgs boson. The relative likelihoods of these zones are estimated by "weighting" them by the (M_H, m_t) probability distribution, whose 1-σ and 2-σ contours are shown as dotted ellipses. We also display the cumulative probability in each zone.
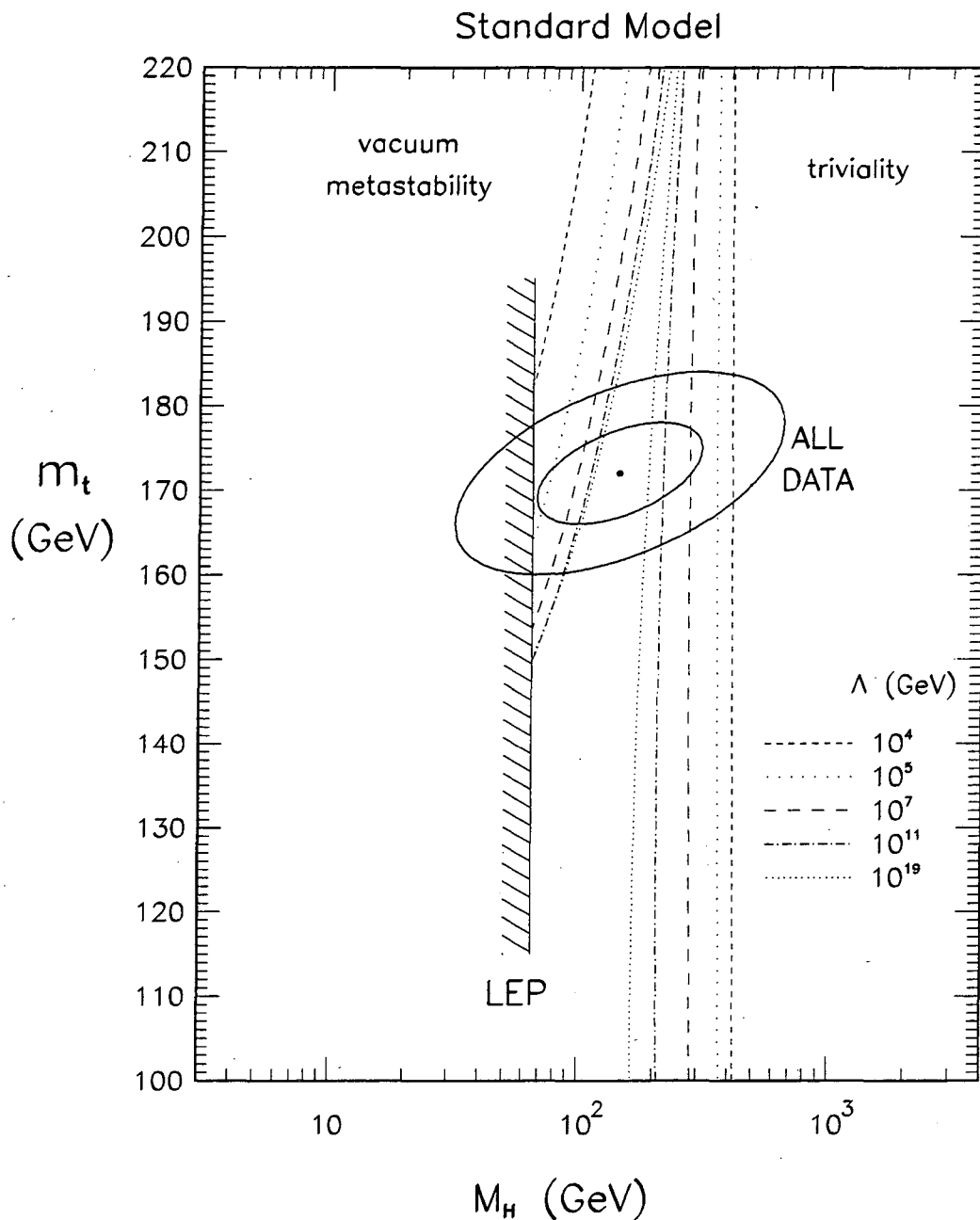
FIG. 1. Indirect bounds on (M_H, m_t) and one-sided experimental and theoretical limits in the Standard Model. The solid ellipses represent the 1-σ and 2-σ contours from the best-fit Gaussian distribution obtained by analysing all electroweak precision data, including the measurement of m_t at CDF and D0. The hatched line is the LEP lower bound on M_H [19]. The other curves represent the lower and upper limits on M_H from vacuum metastability [21] and triviality [22, 23] respectively, as functions of the scale of new physics Λ.
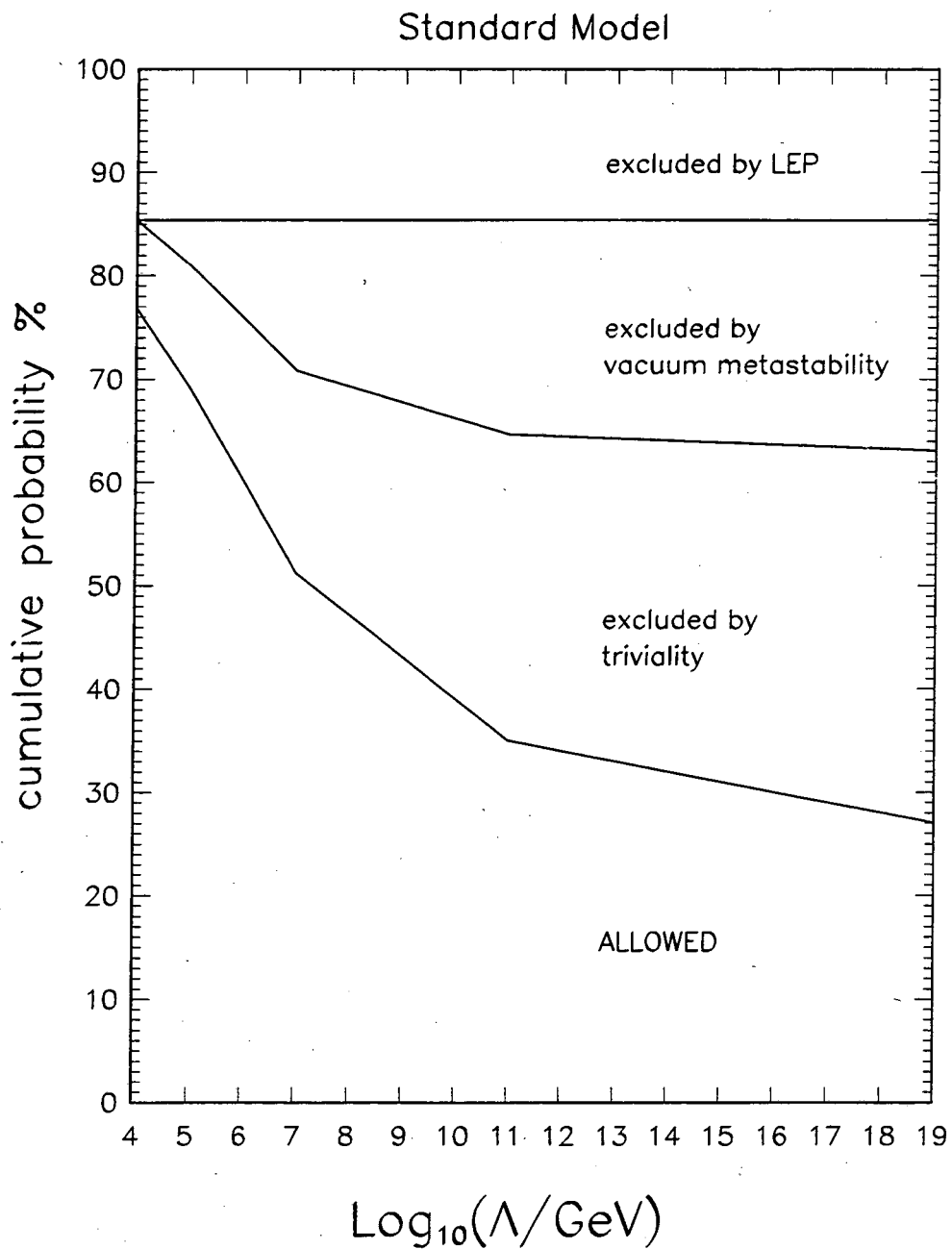
FIG. 2. Cumulative (integrated) probabilities in the various zones excluded or allowed in the Standard Model by one-sided bounds. No value of Λ can be excluded.
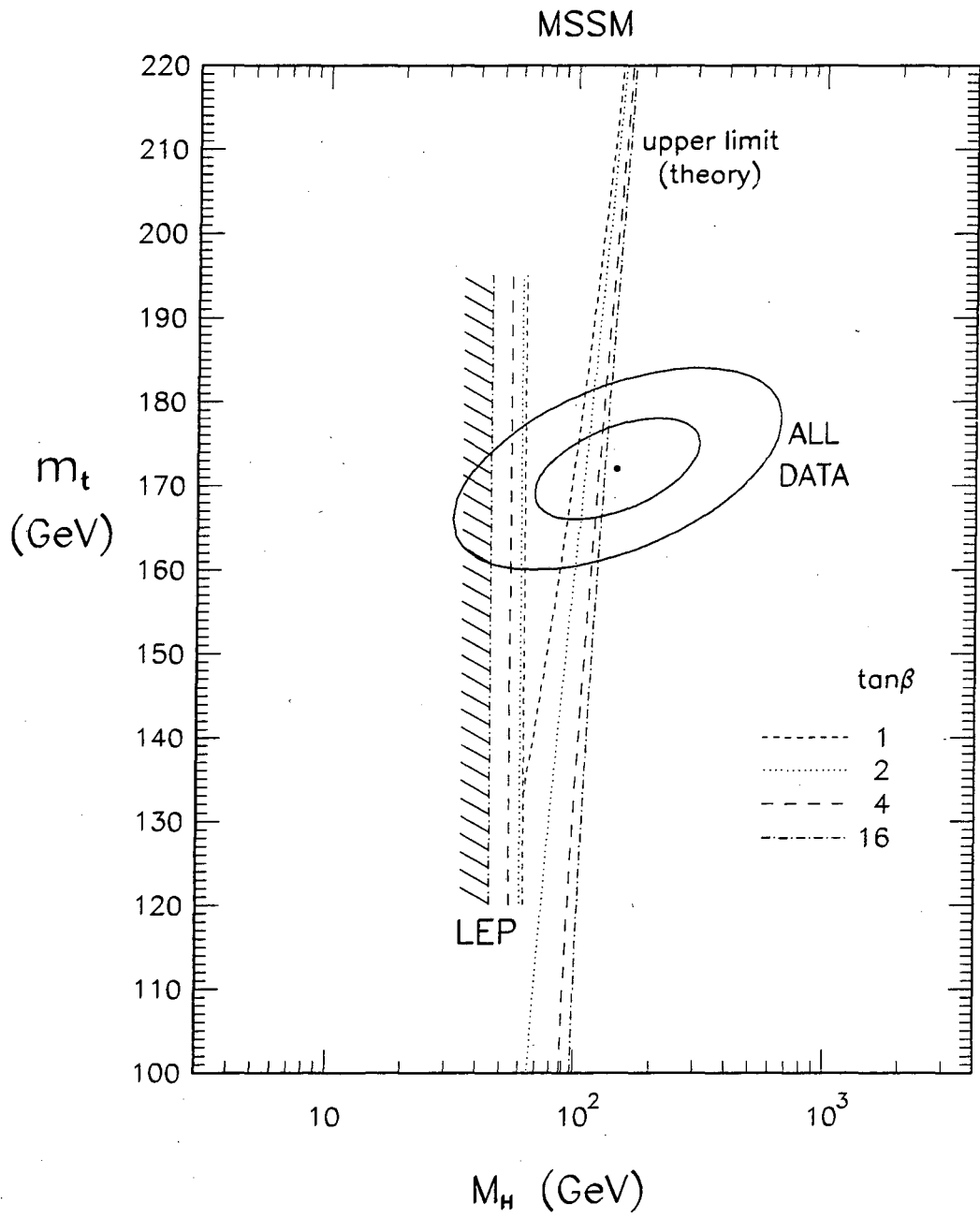
FIG. 3. Indirect bounds on (M_H, m_t) and one-sided experimental and theoretical limits in the Minimal Supersymmetric Standard Model. Apart from the Higgs sector, the MSSM spectrum is assumed to be decoupled. Solid ellipses represent the 1-σ and 2-σ contours as in Fig. 1. The vertical lines are the LEP lower bounds on M_H [20], which depend slightly on $\tan\beta$. The other curves represent the upper limits on M_H in the MSSM [24], as a function of $\tan\beta$.
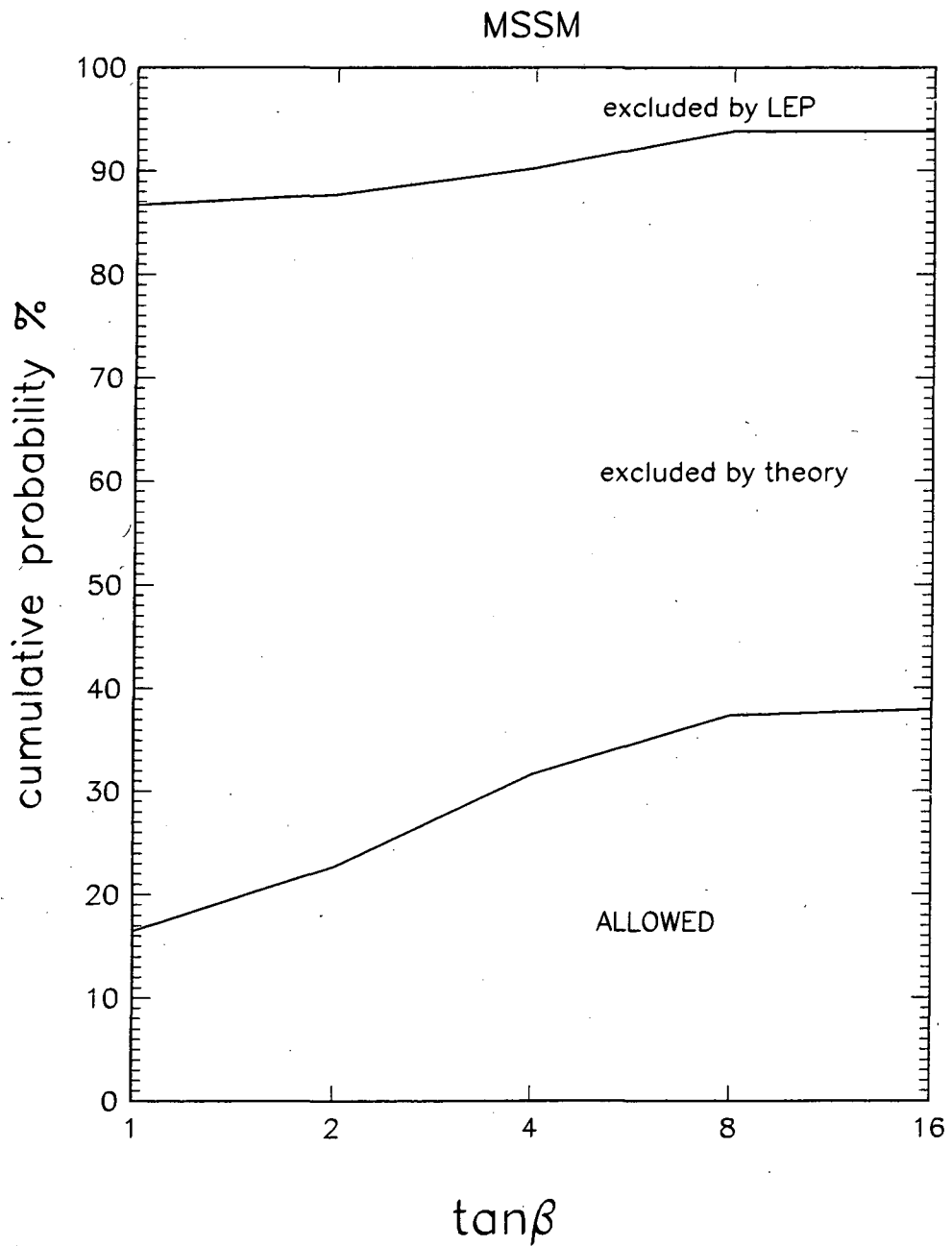
13

FIG. 4. Cumulative (integrated) probabilities in the various zones excluded or allowed in the Minimal Supersymmetric Standard Model by one-sided bounds. No value of tan β can be excluded.
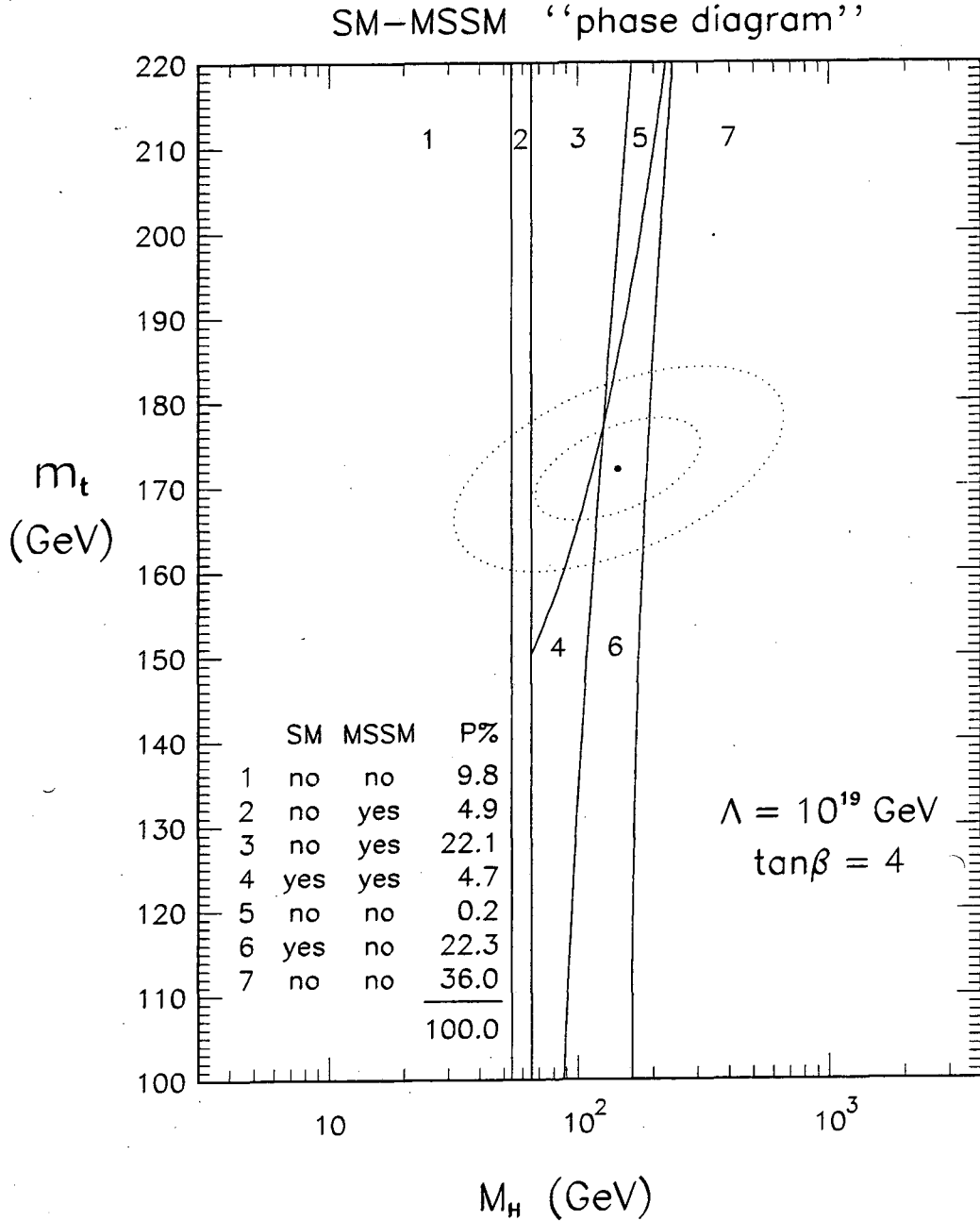
FIG. 5. Superposition of SM and MSSM bounds in the (M_H, m_t) plane, for $\Lambda = 10^{19}$ GeV and $\tan\beta = 4$. The various zones 1–7 define regions that are (not) compatible with a SM or a MSSM Higgs boson. The relative likelihoods of these zones are estimated by "weighting" them by the (M_H, m_t) probability distribution, whose 1-σ and 2-σ contours are shown as dotted ellipses. We also display the cumulative probability in each zone.

ERNEST ORLANDO LAWRENCE BERKELEY NATIONAL LABORATORY
ONE CYCLOTRON ROAD | BERKELEY, CALIFORNIA 94720